Progress in Natural Science: Materials International 2013;23(2):113–126

Chinese Materials Research Society

Progress in Natural Science: Materials International

www.elsevier.com/locate/pnsmi
www.sciencedirect.com

REVIEW

Bimetallic nanostructures with magnetic and noble metals and their physicochemical applications

Sibin Duan, Rongming Wang*

Key Laboratory of Micro–Nano Measurement-Manipulation and Physics (Ministry of Education) and Department of Physics, Beijing University of Aeronautics and Astronautics, Beijing 100191, China

Received 15 September 2012; accepted 13 November 2012
Available online 21 April 2013

KEYWORDS

Bimetallic nanomaterial;
Microstructure;
Synergistic effect;
Magnetic property;
Catalytic property;
Optical property

Abstract Bimetallic nanomaterials consisting of magnetic metals and noble metals have attracted much interest for their promising potentials in fields such as magnetic sensors, catalysts, optical detection and biomedical applications. Bimetallic nanomaterials synthesized by wet-chemical methods with different architectures including nanoparticles, nanowires or nanotubes and their assemblies are summarized in this review. The particular properties of bimetallic nanomaterials, especially their magnetic, catalytic and optical properties, are presented. The advance in electron microscopy makes it possible to understand the nanostructural materials at much higher level than before, which helps to disclose the relationship between the microstructures and properties qualitatively and quantitatively.

1. Introduction

The study of the structures and properties of small particles is a topic which has attracted interest for more than a century [1–3]. The dependence of the properties of nanoscale materials on their sizes, shapes and compositions is a phenomenon of both fundamental scientific interest and technological applications. One important research field in nanoscience and nanotechnology is to design nanomaterials (NMs) with a specific structure and composition through tailor and self-assembly processes at nanoscale. This relies on the knowledge gained from advanced studies of the NMs through specific techniques fostered by synthetic chemists, physicists and material scientists to engage in.

Metal materials are one kind of the most important materials in building modern society [4]. From architecture, transportation equipments, electronic technology, information science and technology to biomedical applications, metal materials are all indispensable constituents [5–7]. Compared with their bulk counterparts possessing high mechanical strength, good malleability and electric–magnetic properties,

*Corresponding author.
E-mail address: rmwang@buaa.edu.cn (R. Wang).

Peer review under responsibility of Chinese Materials Research Society.

Production and hosting by Elsevier

1002-0071 © 2013 Chinese Materials Research Society. Production and hosting by Elsevier B.V. All rights reserved.
http://dx.doi.org/10.1016/j.pnsc.2013.02.001

metal NMs exhibit particular physical and chemical characteristics because of their small-size effect, surface effect and quantum-size effect, and have potential applications in the fields of catalysis, magnetic recording, sensing and medical diagnosis, etc. [8,9]. For example, NMs like Cu, Ag and Au have surface plasmon in the visible light region which can be used as bio-sensor/imaging and opto-electronic devices [10,11]. Some NMs, such as Pt and Pd as well as Ag and Au, have very good catalytic activities. The transition metals, such as Fe, Co, and Ni, are ferromagnetic elements which have been widely used in different magnetic and spintronic devices [12].

Bimetallic NMs, composed of two distinct metal elements, have a certain mixing pattern (or chemistry sequence) and geometry architecture, and perform specific functions [13,14]. They perform not only a simple combination or enhancement of the properties associated with their single counterparts, but also many interesting and surprising new properties with a combination of multiple functions and broadened application fields, which is explained by synergistic effects of NMs [15–18]. By changing their components and morphologies (like core–shell or dumbbell architectures), their relevant physical or chemical performances can be successfully modified [19,20]. The increase of controllable variables leads to inevitable complexity to interpret the interaction mechanism of the bimetallic NMs [13]. Herein, discovering the microstructure nature of their physicochemical properties in the bimetallic NMs system has been attracting great interest of the research scientists.

Among all the metal materials, magnetic and noble metals are two groups of the most prominent materials. Magnetic metal elements (containing Fe, Co, Ni) have two 4s outermost electrons and unsaturated 3d electron shell, which induce rich physicochemical properties, such as specific magnetic and catalytic performances [21,22]. Noble metals mainly contain 4d metals (including Ag, Ru, Rh, Pd) and 5d metals (including Au, Pt). Compared with magnetic metals, noble metals have more profound electron structures, exhibiting irreplaceable advantages in the areas of catalysis and optical detection based on the Surface Plasmon Resonance (SPR) [23,24]. It is of great scientific significance and applied value to combine them together to design new magnetic–noble multifunctional nanostructures, to discover their magnetic responses or catalytic activities and further study the relationship between the properties and the sizes, components and structures of bimetallic NMs [18,20,25–28].

Herein, we will give an overview of bimetallic NMs composed with magnetic and noble metals in different shapes, especially zero-dimensional nanoparticles (NPs) and one-dimensional nanowires or nanotubes in Section 2. The common synthesis methods of bimetallic NMs are also summarized. The recent progress in the characterization technique is presented in Section 3. And in Section 4, we will discuss the unique properties of bimetallic NMs, especially in the magnetic and catalytic fields. The relationship between nanostructures and properties is discussed in detail. In the last section we will analyze the scientific problems and give an outlook in this area based on the previous summary.

2. Various architectures of bimetallic NMs

Bimetallic NMs have great potential in many fields and attract much attention from researchers. Many kinds of bimetallic NMs containing magnetic and noble elements have been synthesized showing diverse shapes or geometry architectures [29]. Wet-chemical method has been proved to be an effective and powerful way for the synthesis of bimetallic NMs by reducing the precursors according to their oxidation–reduction potentials [23,30]. The size and morphology of the obtained NMs can be controlled by utilizing suitable surfactant and coordination compound to control the nucleation and growth processes. Here we summarize the recent progress of the building blocks of bimetallic NMs consisting of zero-dimensional NPs, one-dimensional nanowires or nanotubes and their assemblies.

2.1. *Zero-dimensional bimetallic NMs*

Nanoparticles, as zero-dimensional NMs, are the most common type that can be obtained from wet-chemical synthesis. However, according to their mixing patterns, it can be further classified into three main types as shown in Fig. 1.

In the core–shell NPs, one type of metal forms core and then is fully coated by another kind of metal. Through controlling their core size and shell thickness, their properties can be well modulated (see Section 3).

If the two parts of the bimetallic NMs only share a mixed interface, then the dumbbell shape is obtained. Unlike the case in core–shell shape with only the shell element exposed to environment, the dumbbell shape NMs expose both parts to environment. The performances are often curious and the interface between them plays an important role in controlling their behaviors [31,32].

Different from core–shell or dumbbell structures, the elements of the alloyed NPs are homogeneously mixed randomly or in an ordered manner. The surface variety leads to excellent catalytic activity in the alloyed NPs [33–35].

Various wet-chemical schemes have been applied to synthesize bimetallic NPs. They can be classified into two categories according to the formation mechanisms: co-reduction and sequential reduction methods. The co-reduction method involves reduction of the mixture of two kinds of salts containing the targeted composition using reducing agents. In this case, the oxidation–reduction potentials play a key role to determine the ultimate architecture [36,37]. The sequential reduction method, also called seeded growth in some literatures, reduces one metal (referred to as ''A'') on the surface of the prepared metal clusters (referred to as ''B'') [33,38]. The seed containing B element may be pre-synthesized and then introduced to the solution containing A precursors [39] or synthesized in one pot together whereby A and B elements are reduced at distinct times and/or temperatures in the same liquid medium [38].

In our previous work, nearly monodispersed bimetallic NiPt hollow spheres with an ultrathin shell (2–3 nm) have been successfully synthesized via the platinum catalytic growth strategies [40]. The Pt clusters play a key role in the zero-valent Ni formation, where Ni^{2+} could not be reduced to zero-valent by $NaBH_4$ without Pt. A similar formation mechanism was also proposed in the synthesis of Au–Ni and Au–Co bimetallic NPs [32]. With the combination effect of polyvinylpyrrolidone (PVP) and stirring, the NiPt hollow spheres can be transformed into double-layered NiPt nanobowls through a ''one-pot'' route in water at room temperature without premade templates. The shape of sacrificial Ni

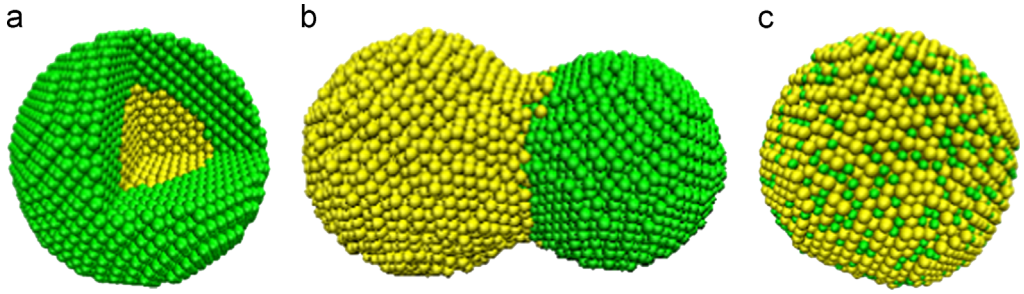

Fig. 1 Schematic illustration of three mixing patterns in zero-dimensional bimetallic NMs: (a) core–shell, (b) dumbbell and (c) alloyed.

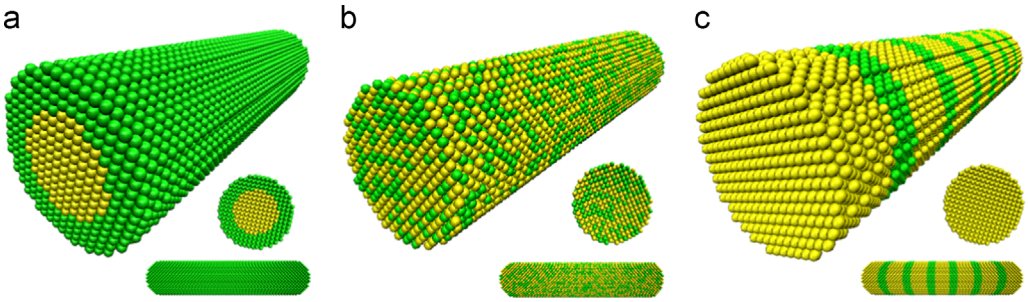

Fig. 2 Schematic illustration of three mixing patterns in one-dimensional bimetallic NMs: (a) core–shell (b) alloyed and (c) bamboo-like.

cores was changed from sphere-like to bowl-like upon introducing rigorous stirring, which determined the morphology of the final products [41].

2.2. *One-dimensional bimetallic NMs*

Similar to zero-dimensional NPs, one-dimensional bimetallic NMs, i.e. nanowires, nanotubes, etc., have three kinds of structures considering the element distribution. As shown in Fig. 2, three kinds of mixing patterns in one-dimensional bimetallic NMs consist of core–shell, alloying and bamboo-like structures. The core–shell structure has a clear interface between the core and the shell. The core can be nanowires, nanotubes, etc. [42]. The two kinds of elements are mixed homogeneously with a certain elements ratio in the alloying nanostructure [43,44]. The two metal elements can also be placed like bamboo to form a one-dimensional structure, where the two kinds of clusters unite alternatively, with elemental distribution anisotropy along the axial direction [45–47].

One-dimensional NMs are often synthesized by using templates. High-density porous alumina template is a common one for the synthesis of nanowire arrays [43,47]. One-dimensional NMs can also be synthesized by using appropriate capping agents to control the growth rates of different directions in a seed [48,49].

2.3. *Bimetallic assemblies*

Depending on the demand of application, the NPs and nanowires or nanotubes can be assembled into various structures such as superlattice and nanochains.

Superlattice can be assembled by monodisperse NPs with size distribution less than 5% in the form of close-packed arrays on a variety of substrates. The particles are linked by van der Waals, weak hydrogen bond and electric–magnetic interaction. Superlattice with variable lattice parameter can be obtained by controlling these driving forces, such as adapting appropriate solvent and organic capping agent or controlling the solvent evaporation conditions. FePt superlattice can be achieved by spreading monodisperse FePt NPs on a substrate with oleic acid and oleylamine as stabilization and oxidation-preventing agents and evaporating the carrier solvent slowly [50]. The driving force comes from van der Waals and magnetic interactions. To control the superlattice parameter, surfactant exchange on the surface of the particles is performed before the self-assembly. Fig. 3(a) shows the superlattice assembled by FePt NPs coated with oleic acid and oleylamine, while Fig. 3(b) shows the NPs coated with hexanoic acid/hexylamine. The interparticle spacing in Fig. 3(a) is around 5 nm. That is twice as wide as the distance given by the C18 chain (~2.5 nm) in the oleic acid and oleylamine molecules, while in Fig. 3(b) the interparticle spacing is closer to 1 nm due to the thin-layer coating on the particles.

Another kind of assembly form is that of nanochains constructed from nanospheres. And the building blocks usually contain magnetic element such as Fe@Au [51], Co@Au [52]. Compared to other building blocks, magnetic NPs have an additional magnetic force, which favors the formation of magnetically aligned chains of magnetic dipoles, rather than two- or three-dimensional structures. In our group, we have carried out a series of investigations on the Ni nanochains by external magnetic fields induced method formation before [53–57]. More recently, by applying magnetic fields as manipulating method, CoPt hollow nanochains were obtained [58]. The results indicate that the length of the CoPt hollow nanochains can be controlled by magnetic fields, the same as cases in the Ni nanochains (Fig. 4). The phenomenon suggests that magnetic field can act as effective manipulation method in the synthesis of one-dimensional magnetic NMs.

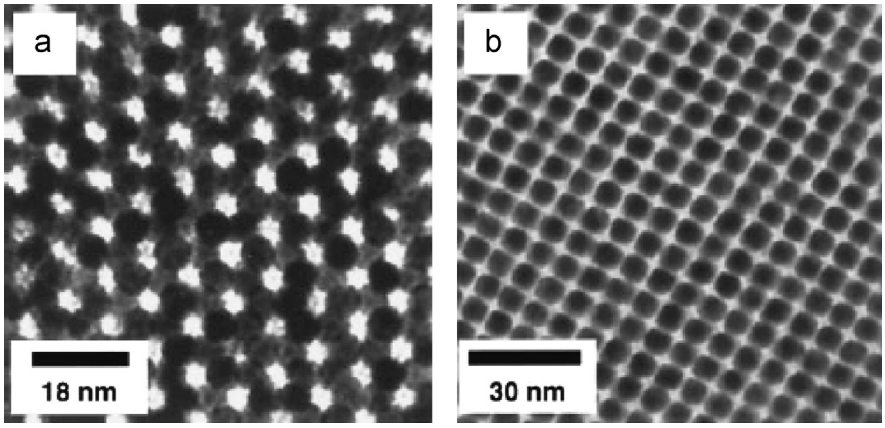

Fig. 3 Transmission electron microscopy (TEM) images of a 3D assembly of 6-nm as-synthesized $Fe_{50}Pt_{50}$ particles coated with (a) oleic acid/oleylamine or (b) hexanoic acid/hexylamine [50].

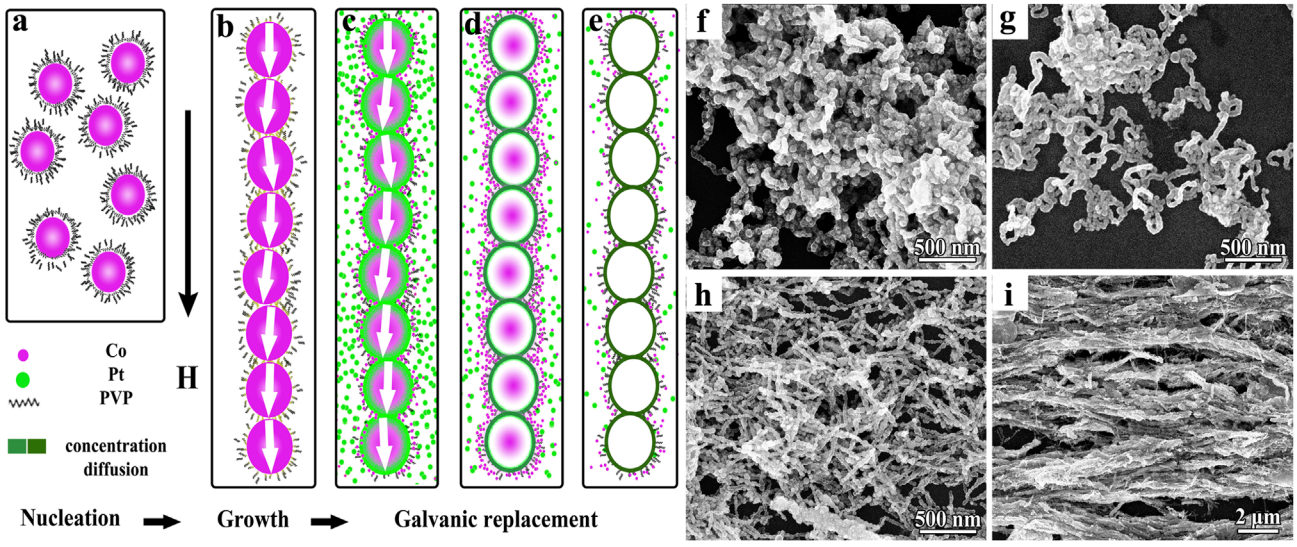

Fig. 4 Schematic formation of CoPt hollow nanochains (a–e). (a) Formation of Co particles in PVP solution. (b) Growth and formation of Co nanochains covered with PVP under magnetic fields. (c) Galvanic replacement between Co atoms and Pt ions. (d) Diffused Co ions capped by PVP molecular and reduced together with Pt ions. (e) CoPt hollow nanochains formation after the replacement; SEM images of the CoPt products synthesized under magnetic fields of (f) 0, (g) 0.5, (h) 2 and (i) 8 kOe [58].

3. TEM advantages in the characterization methods

The structures of the bimetallic NMs can be much more complicated compared to the monometallic NMs. Besides the size, shape, twinning [59] and morphology, there are some other structure elements for the bimetallic NMs. In a bimetallic system, there may be order–disorder transition [60] and strain [61] in the bimetallic NMs.

To characterize the structure of a bimetallic system, a wide range of techniques has been employed. These techniques include microscopic techniques, such as X-ray photoelectron spectroscopy (XPS), X-ray absorption spectroscopy (XAS), X-ray diffraction (XRD), nuclear magnetic resonance (NMR), focused ion beam (FIB) [62], etc. Although these techniques have given us valuable information, these techniques do not appear accurate enough to study the detailed structure especially for really small NPs; for example, XPS is not strictly surface specific and the detected signal intensity is a superposition originating from a number of atomic layers, yielding some average composition throughout the characteristic probing depth. XAS (EXAFS and XANES) as well as other spectroscopic techniques can only give averaged results in a whole sample that is always not the case for bimetallic NMs. So to obtain fruitful crystal and electronic structure information of a nanoparticle, more efficient techniques, by which combined high resolution microscopy and spectroscopy can be performed simultaneously at ultra-high resolutions, are required. Traditional TEM based techniques have also been widely used in bimetallic NMs research. For example, recently, CoPt bimetallic NPs were studied using combined nanobeam electron diffraction and HREM. It was proved that the size and shape can have effect on the order–disorder phase transition [60]. The current proposer has studied Cu–Pd/γ-Al_2O_3 catalysts using combined high angle annular dark field (HAADF) performed in scanning transmission electron microscopy (STEM) mode and electron energy loss spectroscopy (EELS) and energy dispersive spectroscopy (EDS) at high spatial resolutions [63]. Clear element distributions of Cu and

Pd elements in the bimetallic NPs have been obtained, whereas, due to the limitation in both spatial and energy resolution, the surface and interface structure have not been well defined yet. Nevertheless, the results clearly demonstrated that HAADF imaging combined with EELS or EDS is a suitable technique for the study of the detailed structure and chemistry of the metallic NPs.

During the past several years, great progress has been made toward microstructure characterization tools, among which, aberration corrected electron microscopy (ACEM) has been successfully used for the study of feature size down to sub-Angstrom region [64]. These types of ACEM can be used for mapping element distribution using EDS at very high spatial resolution besides their ability to directly study the behavior of a single atom. These advanced instruments help to enhance our understanding of nanostructural materials at much higher level than before. There are a couple of reports on the applications of such ACEM in the study of NMs. Strasser et al. studied PtCu bimetallic NPs using an ACEM and revealed the core–shell nature of the NPs directly. They also calculated the strain inside the nanoparticle based on the data acquired from both ACEM and anomalous X-ray diffraction (AXRD) [61] and generated a relation between reactivity and strain that provides guidelines for tuning electrocatalytic activity. Although the AXRD data can only give the average lattice parameters and average composition of the NPs, their finding that electrocatalytic activity can be tuned by control the stain in the nanoparticle has opened a way to tune other strain related properties of the NPs. Considering the inhomogeneous nature of most bimetallic NMs, more localized TEM based techniques will work better than AXRD in strain measurement [65,66]. Mayoral et al. studied the interface structure in Co–Au bimetallic NPs using ACEM [67]. They found that the as-synthesized NPs, that have initially core–shell bimetallic structures, have changed to a structure with a fine Co layer forming a perfect interface with the gold after thermal treatment at normal atmospheric conditions. The ordering of the Co-rich zone presents a face-centered cubic (fcc) arrangement matching the gold lattice.

Besides qualitative study, quantitative study is becoming a main trend in characterizing the structure of NMs due to advances in both instrumentation and software. For example, Pd-core and Pt shell nanodiscs were studied using a STEM revealing that a thin, uniform Pt shell was formed around the Pd nanoplate, and demonstrating the layer-by-layer epitaxial growth of Pt on Pd surface in this approach [68]. Also using an ACEM, Ferrer et al. studied Au–Pd bimetallic NPs and found the existence of some nanosized defects in the surfaces, such as steps and entanglement [69]. In our previous work, the periodic shell structure and surface reconstruction of bimetallic FePt NPs with icosahedral structure have been quantitatively studied by high-resolution TEM with focal series reconstruction with sub-Angstrom resolution, confirming the Fe-rich core and Pt-rich shell, as shown in Fig. 5 [70,71]. Localized lattice relaxations have been studied by extracting the position of individual atomic columns with a precision of about ± 0.002 nm. The lattice spacings of (111) planes from the surface region to the center of the icosahedra are found to decrease exponentially with shell numbers. Computational studies and energy-filtered transmission electron microscopy analyses suggest that a Pt-enriched surface layer is energetically favored and that site-specific vacancies are formed at the edges of facettes, which was experimentally observed [72]. For bimetallic NPs, composed of a magnetic metal element and a noble metal element, there is a problem measuring their compositions using EELS (except FePd) because both Pt and Au do not give distinct EELS peaks, whereas, EELS can give chemistry information of the magnetic metals in the NMs. EDS that can be performed at very high spatial resolution is needed to measure the compositions of the systems. Braidy et al. have developed a method for quantitative EDS micro-analysis of some alloyed NPs [73]. Combined EELS and EDS analysis together with HAADF imaging should be able to give both composition and chemistry information of the bimetallic NPs at very high spatial resolutions using an ACEM.

NMs owing to their small size, high aspect ratio and high activity tend to undergo sintering and thus lose their characteristic properties. Lim et al. using a special TEM holder purchased from Protochips Inc. [74] demonstrated the ability to study the behavior of monometallic NPs at atomic

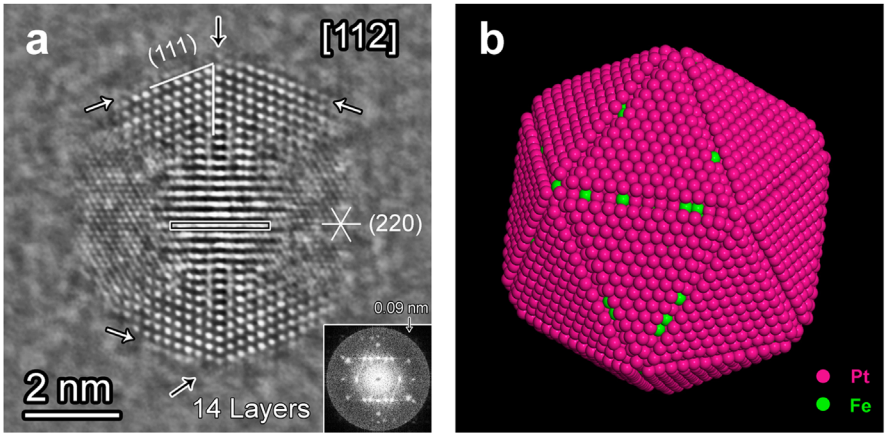

Fig. 5 Experimental image and proposed model of the FePt nanoparticle. (a) Experimental exit wave phase images of the representative FePt nanoparticle. White arrows mark partially occupied shells. Dark arrows mark edge columns that are commonly missing. The inset of (a) is a Fourier transform of the phase image showing an information limit of 0.090 nm. (b) Proposed icosahedrons with 10,179 atom sites and Pt atoms that segregated to the surface (pink). Edge atom columns are removed making some of the (green) iron atoms of the second shell visible [70].

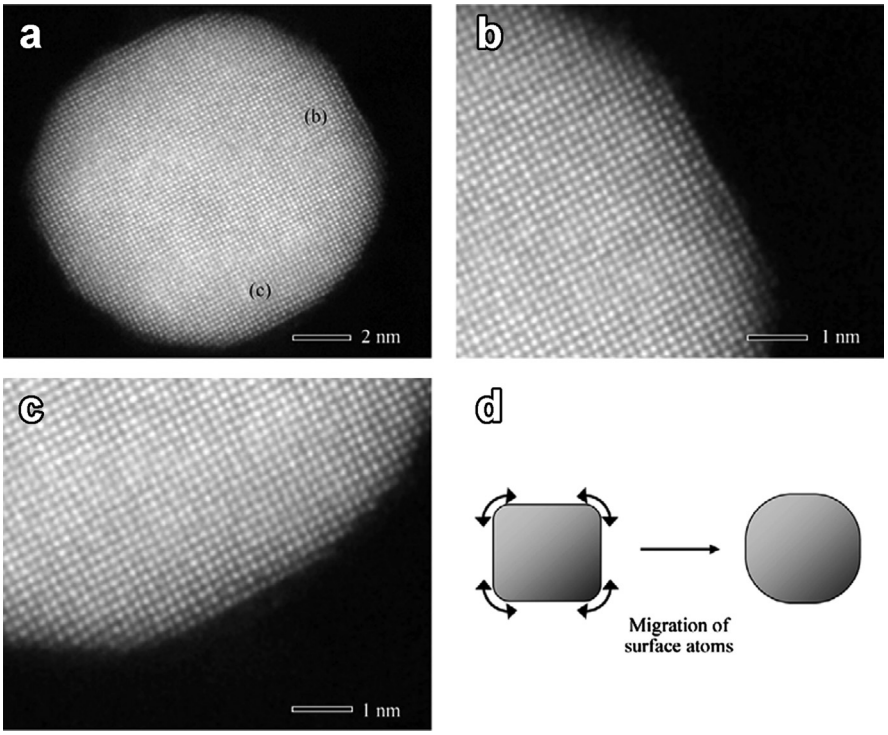

Fig. 6 (a) HAADF-STEM image taken from a Pd nanobar supported on a carbon film after in situ annealing inside the electron microscope chamber at 500 °C for 1 h. (b, c) Magnified images of the selected regions in (a). Individual Pd atoms are resolved as white spots. (d) Schematic illustration of the migration of surface atoms during the annealing process [75].

resolution at high temperatures (~1000 °C) (see Fig. 6) [75]. There is a critical need for in-situ study of bimetallic NMs for the determination of their stability (segregation of metal components) under different conditions. Metal NMs with precisely controlled size and composition are highly attractive for heterogeneous catalysis. However, their poor thermal stability remains a major hurdle in the way toward application at realistic technical conditions. Recent progress in this area has focused on nanostructured oxides to stabilize embedded metal NMs. For example, an alternative approach that relies on synthesizing bimetallic NPs with precise compositional control to obtain improved high-temperature stability was reported [76].

4. Structure–property relationship of bimetallic NMs

Nanomaterials, for their small size, exhibit very fantastic properties [77,78]. In order to explain the interesting phenomenon, classical physical laws might be no longer suitable. As for bimetallic system, because of the introduction of another component, the system became much more complex. The interaction between the two metals greatly influences the performances. The united section combining two different metals has a strong chemical bonding, which will obviously change localized electron structure resulting in various and interesting chemical and physical properties. At a fundamental level, information on the evolution of electronic structures and their effects on the catalytic, optical and magnetic properties continue to be a major goal of research in bimetallic NMs. On a practical level, the unique catalytic, optical, and magnetic properties of bimetallic NMs are exploited for a variety of applications including enhanced catalytic activity and selectivity [79], fine tuning of optical properties [80], magnetism [50], drug delivery [81] and electronic materials [82]. It was found that the formation of the FePd alloyed particles in a Pd/CeO_2 shows enhanced activity for water–gas shift [83]. The PdM, PtM and AuM (M = transition metals) alloyed NPs represent rich systems with several important applications in catalysts and magnetic materials. Both FePd and FePt are ideal materials for permanent magnetic applications because of their large uniaxial magnetocrystalline anisotropy and good chemical stability [84]. Alloying Pt with magnetic metals, like CoPt, FePt or NiPt, has been identified as a possible method to mitigate some of the cost (and performance) issues associated with Pt electrocatalysts that have been widely used in proton-exchange membrane fuel cells (PEMFCs) [85].

More recently, a new concept has been presented by Temnov et al. [86]. Combining magnetic and plasmonic counterparts in a magneto-plasmonic system would both enable high magneto-optical activity and support propagating surface plasmon modes. Orders of magnitude smaller external magnetic fields might be sufficient to manipulate the optical properties of their surface plasmon polariton (SPPs). The concept allows the design and tailoring of the optical properties of complex composite magnetic materials toward particular potential applications such as high sensitivity bio-sensing devices [87]. This is an exciting and very interesting area to work with. However, there are only some limited reports on this topic.

Here, we will focus on the magnetic, catalytic and optical properties of bimetallic NMs, which critically depend on their size, morphology, composition and surface interaction.

The relationship between the properties and nanostructures is discussed.

4.1. Magnetic properties

Magnetic NMs exhibit great potential applications such as magnetic data storage [26,88–90], microwave absorption [91,92], magnetic fluid [93,94] and biomedicine [95–97]. The performances of magnetic NMs are critically dependent on their magnetic features, containing temperature dependent blocking temperature (T_b), field dependent coercivity (H_c) and saturation magnetization (M_s). For bimetallic system, the magnetic property is strongly dependent on the interparticle and intraparticle interaction, which can be controlled by their elements type, ratio, distribution and their geometry architecture.

Magnetic bimetallic NMs, consisting of two kinds of magnetic elements such as Ni–Co [98,99] or Fe–Ni [100,101], Fe–Co [20,102–104] NPs, have been investigated by many researchers. Through controlling their component or morphology, the magnetic properties could be well manipulated. For Ni–Co core–shell NPs synthesized by Ni-catalyzed method under microwave irradiation, the magnetic behaviors of Ni, $Ni_{50}Co_{50}$, $Ni_{33}Co_{67}$, and carbon-coated Co nanopowders are all ferromagnetic, but the values of saturation magnetizations at 300 K are different: $Ni_{50}Co_{50}$ and $Ni_{33}Co_{67}$ are 90.7 and 99.7 emu g^{-1} at 300 K, respectively, and larger than that of Ni (48.6 emu g^{-1}), that is the value increases as the Co content increases (M_s (bulk fcc Ni): 55.1 emu g^{-1} and M_s (bulk hcp Co): 161.9 emu g^{-1} at 293 K), as is shown in Fig. 7 [98].

Moreover, introducing noble metal to form magnetic–noble bimetallic NMs is another method to manipulate their magnetic performances. Many previous works have demonstrated that the presence of noble metal leads to high magnetic anisotropy as well as high saturation magnetization and coercivity, showing promising applications as microwave absorber, magnetic recording media and drug deliverers [19,47,97,101,105,106]. Massive fabrication of free-standing Co/Pt magnetic barcode nanowires with well-defined interfaces and layer thicknesses was carried out with high-density porous alumina templates [47]. Any desired barcode with different sequences and thicknesses could be fabricated easily by changing the deposition time. The ferromagnetism of these barcode nanowires can be modulated easily by changing the thickness of cobalt segments as is shown in Fig. 8. The coercivity (H_c) of the nanowires initially increases rapidly with an increase in the aspect ratio of the cobalt segments to platinum segments (referred to as "γ") but then approaches saturation. While γ is 45, the coercivity measured with external field parallel to the axis of the nanowires is the largest (668 Oe), and Hc decreases with the decrease of γ. The results indicate that nanowires with high shape anisotropies could produce large coercivity. Moreover, by simple further thermal annealing, to form alloyed interface between the cobalt segments and platinum segments, enhancements of the ferromagnetism of Co/Pt barcodes with larger coercivity under both parallel and perpendicular fields can be obtained.

Park et al. also pointed out that the anisotropic phase transitions play an important role in the magnetic behaviors of bimetallic NMs [107]. The fcc Co@Pt core–shell NPs exhibit superparamagnetism at room temperature ($H_c=0$). After the annealing process at 700 °C to anisotropic face-centered tetragonal (fct) structure, the magnetic coercivity of the NPs is significantly enhanced from 0 to 5300 Oe exhibiting room-temperature ferromagnetism, overcoming the superparamagnetic limitations of common magnetic nanomaterials (Fig. 9).

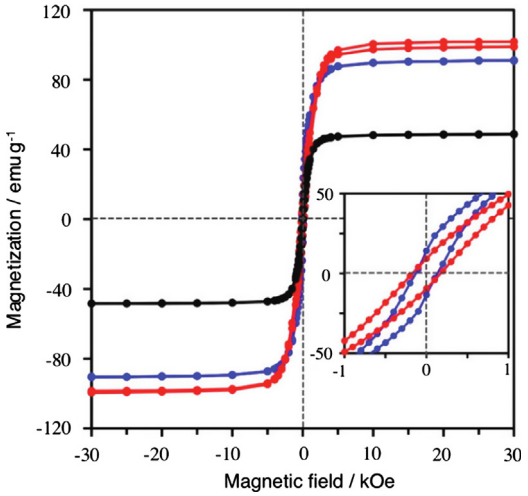

Fig. 7 Magnetization versus applied field for $Ni_{50}Co_{50}$ (blue), $Ni_{33}Co_{67}$ (red), and Ni (black) at 300 K. Inset shows a close-up of the region around zero [98].

4.2. Catalytic properties

Another important application of bimetallic NMs is in the field of catalysis. Magnetic and noble metals all have complex electron structures, exhibiting promising potential in the field of catalysis containing electrochemical catalysis, heterogeneous catalysis, and photochemical catalysis. Bimetallic NMs have been proved to possess better catalytic activity, selectivity and stability for the synergistic effect. In our previous work, alloyed NiPt hollow spheres exhibit excellent electrocatalytic activity and stability [40]. Ren et al. found that Ni–Pt bimetallic catalyst demonstrated the highest activity to CO oxidation, where 100% CO conversion occurs near room temperature. The synergistic effect between platinum and nickel was proved [18].

As known to all, the specific sites on the surface of catalysts play a key role to determine different molecular reactions. In the catalyst field, pursuing perfect selectivity is one of the main research targets as well as high activity and stability. For the purpose of enhancement in the reaction selectivity, factors such as dimension, morphology, and structure, which are bound up with surface sites, need to be regularly controlled. In the selective hydrogenation reaction, bimetallic NMs are proved to possess superior catalytic properties than their single counterparts. Pt NPs with different dimensions have been demonstrated to exhibit distinct difference in the cinnamaldehyde hydrogenation, where their selectivity to cinnamyl alcohol increases with their dimensions [108]. According to the result of theoretical calculation, flat surfaces adsorb the cinnamaldehyde in a different mode with low coordination sites (such as corners, kinks, adatoms, and defective sites), forming different molecular orbitals, which account for different selectivities. The fraction of low coordination sites

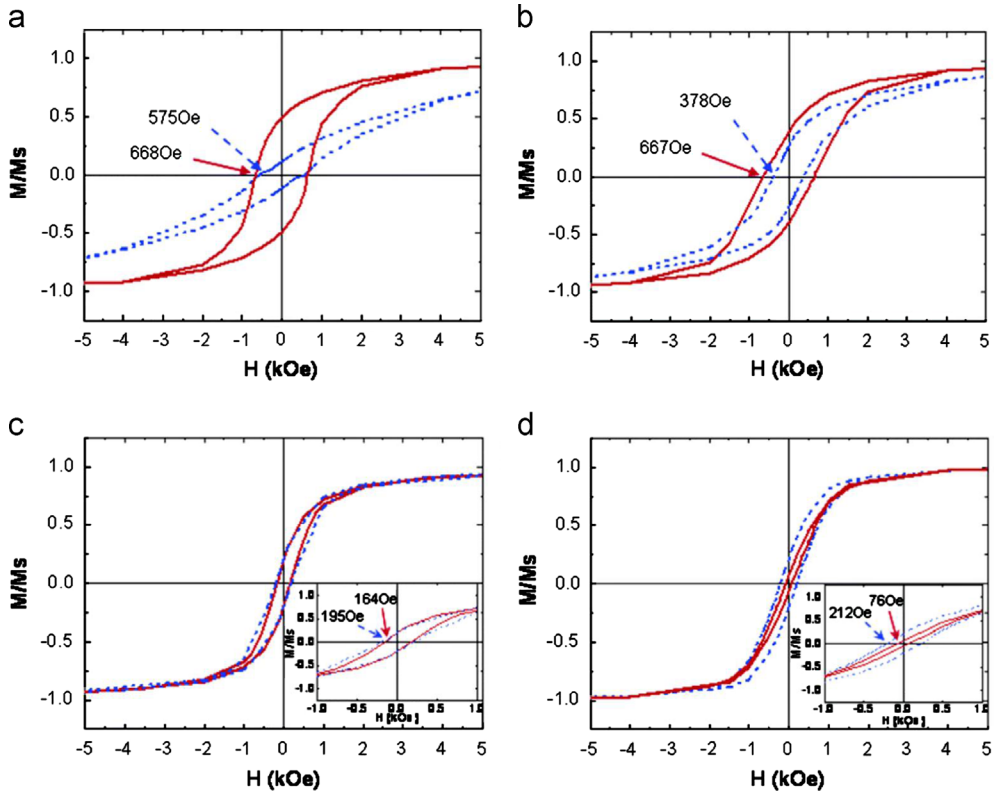

Fig. 8 Magnetic hysteresis loops of Co/Pt magnetic barcode nanowires at 300 K with applied field parallel (//) to the nanowires (solid line) and perpendicular (⊥) to the nanowires (dashed line). (a) Pure Co nanowires, Co/Pt magnetic barcode nanowires with (b) aspect ratio of 3.7, (c) aspect ratio of 1 and (d) aspect ratio of 0.28 [47].

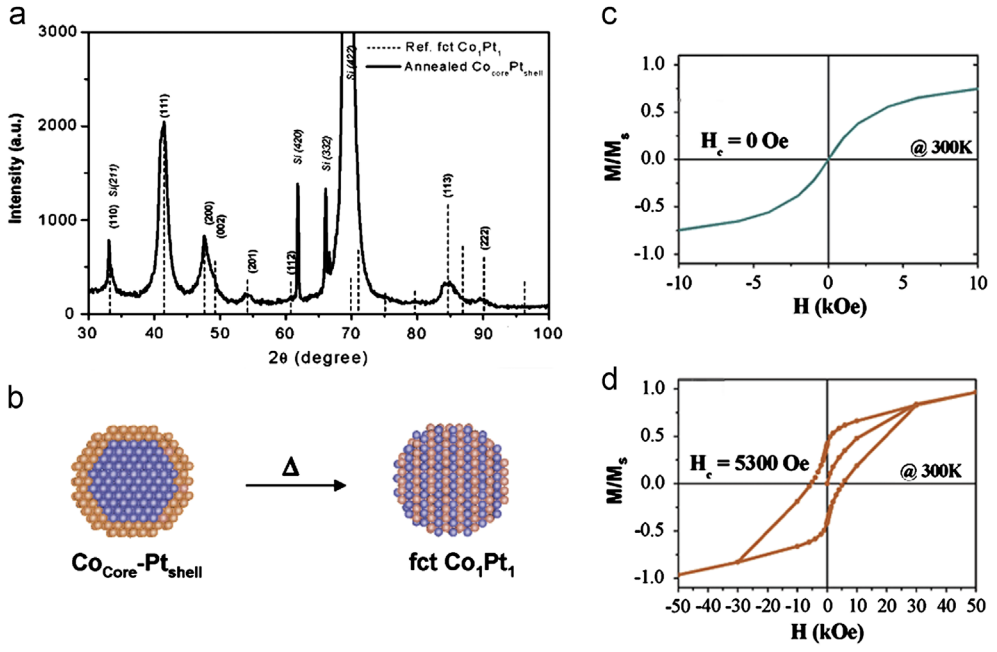

Fig. 9 Magnetocrystalline phase effects on magnetism: (a) XRD pattern of Co@Pt core–shell NPs annealed at 700 °C for 12 h. All peaks are well matched to reference fct Co1Pt1 alloys (dashed line). (b) Thermal alloying of Co@Pt core–shell NPs to anisotropic fct structure. Hysteresis loops of (c) fcc Co@Pt core–shell NPs and (d) fct CoPt nanoalloys measured at 300 K [107].

decreases with the increase in the size of Pt crystals, thus resulting in a corresponding increase in the selectivity to the unsaturated alcohol. However using larger unmodified Pt crystals cannot further raise the selectivity to 100%. And larger crystals will reduce the economical efficiency. The effect of Co atoms decorated on these Pt crystals was then studied.

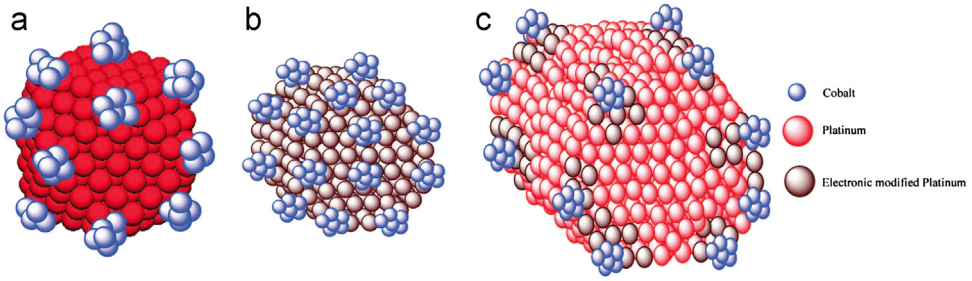

Fig. 10 Pictorial models accounting for the critical size effect: (a) model showing Co atoms decorating on corner sites of Pt crystal. Models accounting for the critical size effect: (b) Co atoms decorated on corners electronically influencing the whole small Pt ensemble—left and (c) some normal Pt sites remained without being influenced by decorated Co atoms in a large Pt ensemble [108].

The results indicate that the decoration of Co atoms on the surface low coordination sites changes the electron structure of Pt NPs, which leads to the increased activity of C═O hydrogenation and suppression of C═C hydrogenation, realizing the high selectivity (up to 99.7%), and it is critically dependent on the molar ratio of Co/Pt elements and the size of Co-decorated Pt nanocrystals is as shown in Fig. 10.

For the catalytic reactions, alloyed NPs possess superior catalytic properties to their single counterpart, derived from specific surface active sites. In many cases, alloying component that cannot be obtained in bulk materials will be realized at nanoscale. It is because, as the dimension decreases, the gap between energy levels that cannot be compounded becomes narrower with the transformation of electron structures. Meanwhile, through surface detection with the help of XPS technique, bimetallic NP catalysts have been proved to undergo surface composition segregation. Driven by different oxidizing and reducing chemical environments, the composition and chemical state reversibly change. Thus, the concept of "smart" catalysts whose structure changes advantageously depending on the reaction environment was proposed [27]. Rh–Pd and Pt–Pd core–shell NPs have been demonstrated to undergo restructuring driven by reaction conditions, while $Pd_{0.5}Pt_{0.5}$ does not. At different photon energies (645 eV, 850 eV, 1486 eV), Rh 3d and Pd 3d photoelectrons excited at the depth of approximately 0.7, 1.0, and 1.6 nm can be detected. From photoelectron spectrum detected under different sources (645 eV, 850 eV, 1486 eV), 0.5 nm $Rh_{0.5}Pd_{0.5}$ nanoparticle was identified as Rh surface segregation "core–shell" nanostructures. The same result was obtained in 0.5 nm $Pt_{0.5}Pd_{0.5}$ nanoparticle. The atomic fractions presented in Fig. 11 were obtained with an X-ray energy of 645 eV and thus represent the changes in composition in the 0.7-nm shell. After oxidation by NO, the Rh in the shell was 94% oxidized. Then after CO was added, the catalytic reaction NO+CO→ N2+CO occurred, while the surface Rh fraction decreased to 0.46, and the Pd fraction increases to 0.54. This result indicates that a drastic restructuring of the shell and core of the NP took place, where Pd migrated to the shell and Rh migrated to the core. If CO was removed then, Pd migrated to the core, Rh to the shell and was oxidized, that is, atom distribution and chemical state are reversible and dependent on the surrounding reactive gases. The reversible core–shell structure responding to the surrounding gases is because of the lower surface energy of Pd relative to Rh and the fact that the Rh oxide is more stable than the Pd oxide.

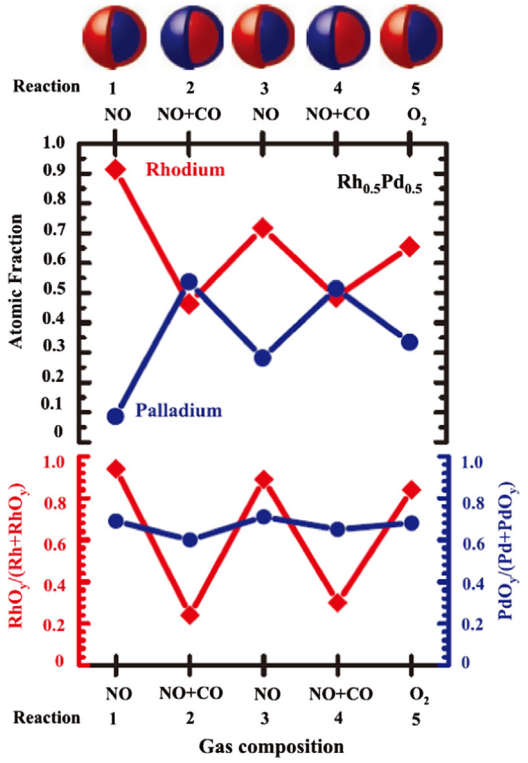

Fig. 11 (Top) Evolution of Rh and Pd atomic fractions in the $Rh_{0.5}Pd_{0.5}$ NPs at 300 °C under oxidizing conditions (100 mTorr NO or O_2) and catalytic conditions (100 mTorr NO and 100 mTorr CO) denoted in the x axis. (Bottom) Evolution of the fraction of the oxidized Rh (left y axis) and Pd atoms (right y axis) in the examined region under the same reaction conditions as the top part of the figure [27].

These results indicate that bimetallic NPs exhibit great flexibility and adjustability in catalytic reactions.

Besides, the same phenomenon in which electron structure as well as geometry structure underwent reversible change was also observed in the other kinds of bimetallic NMs such as CoPt NPs, where the oxidation states of Co atoms in CoPt NPs are altered as the reaction conditions [109]. Furthermore, Co is much easier to be reduced when alloying with Pt atoms.

Multilayer core–shell nanostructures, compared to the simple core–shell nanostructures, can further improve the catalytic properties for the electron structures change induced by strong coupling effect between multiple element atoms. Au@Pd@Pt triple-layered core–shell structured NPs

consisting of a Au@Pd core and nanoporous Pt outer shell were obtained through a simple, rapid, one-step synthesis method [110]. And the electrochemical catalysis measurement indicated that Au@Pd@Pt triple-layered structure has superior catalytic activity toward methanol oxidation compared to Au@Pt structure.

4.3. *Optical property*

Apart from the applications in the field of magnetism and catalysis, bimetallic NMs show great potential application in SPR. For Au–Ag nanocages with controllable pores on the surface, SPR peaks change with the size and locations of the pores [111]. With the growth in number of pores, the extinction peak of Au–Ag structures using Ag nanocubes with sharp corners as sacrificial template was continuously red shifted from 478 nm (blue color) to 650 nm (pink), 770 nm (red), and 870 nm (colorless). However, using Ag nanocubes with truncated corners as sacrificial template, the pores would become more regular and better controlled. In this situation, the number of SPR bands was reduced and the main peak was blue shifted (as shown in Fig. 12). Meanwhile, the phenomenon that SPR peak is not only related to the morphologies of the product (hollow or porous structure), but also connected with the composition was observed in AgAu nanocage structure [112]. The result indicated that as the ratio of Au element increases, the peak is red shifted.

Bimetallic NMs also exhibit great enhancement in the Surface Enhanced Raman Scattering (SERS). Tian et al. conducted a series of investigations into the SERS capabilities of core–shell bimetallic NMs and found that Au–Pd core–shell NPs greatly enhanced the SERS activity with the Pd shell. The enhancement factor of the ultrathin Pd shell was found to be over 5×104 [113]. Au@Ag core–shell NMs were also proved to present higher SERS capabilities than Au, Ag, and Ag@Au NPs [114].

5. Conclusions and outlook

The area of bimetallic NMs synthesis and characterization has undergone tremendous expansion over the past few years. As highlighted in this review, bimetallic NMs including NPs,

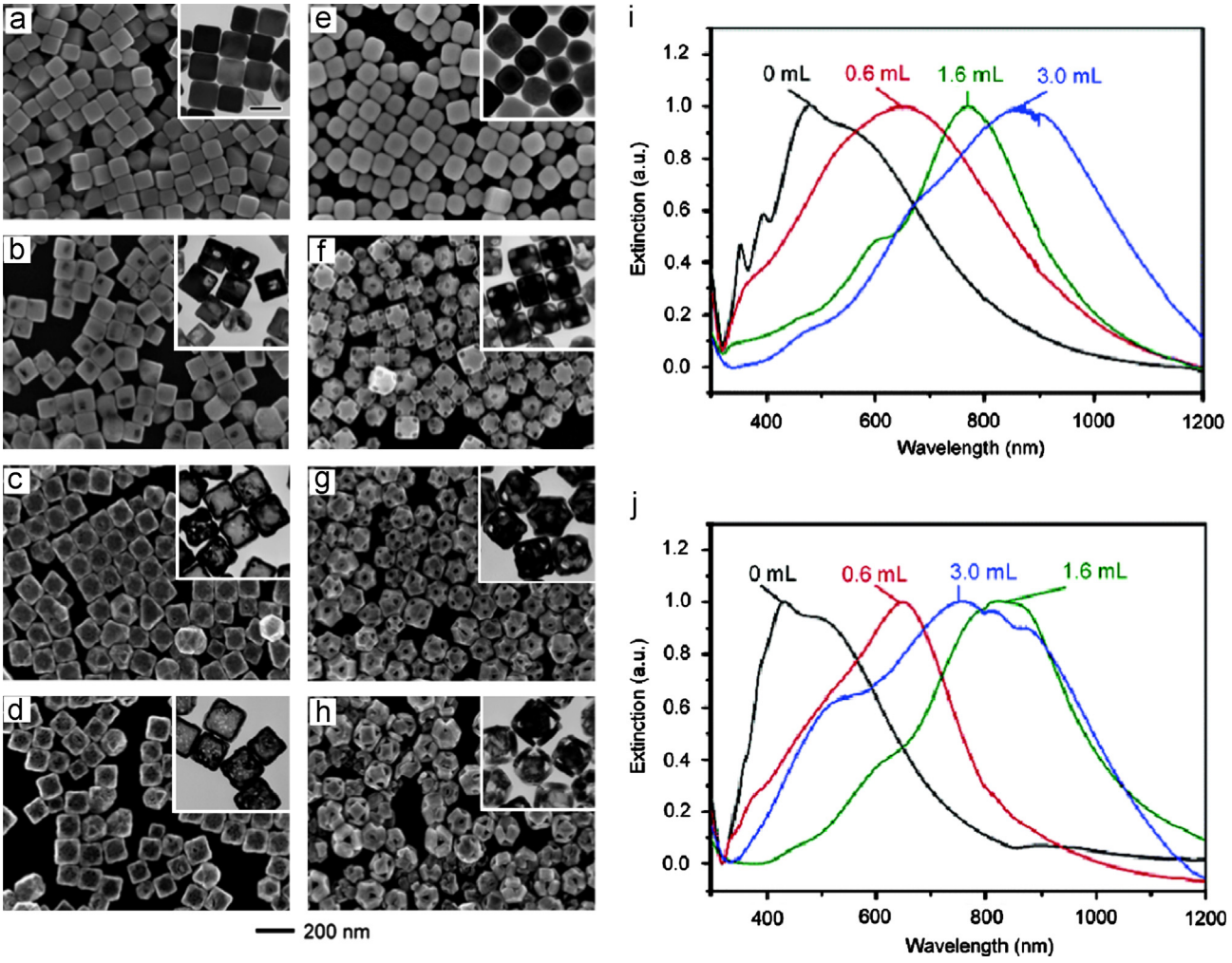

Fig. 12 SEM images of (a–d) Ag nanocubes with sharp corners titrated with 0.1 mM $HAuCl_4$, 0, 0.6, 1.6, and 3.0 mL. (e–h) Ag nanocubes with truncated corners reacted with the same volumes of 0.1 mM $HAuCl_4$ as for the sharp cubes. (Inset) TEM image of each respective sample. Scale bar = 100 nm for all TEM images; UV–vis–NIR spectra of two different types of Ag nanocubes: (a) Ag nanocubes with sharp corners, and (b) Ag nanocubes with truncated corners [111].

nanowires, nanotubes and their assemblies exhibit superior magnetic, catalytic and optical properties compared to their single counterparts. And the performance is critically related to their dimensions, morphologies, mixing patterns, element distributions and especially surface electron structures. By controlling these factors, the properties can be well adjusted, which show excellent potential in the applications such as magnetic data storage, optical detection, sensors, bioseparation and drug delivery.

However, the relationship between structure and property is also qualitative in the previous work, lacking in the atom level and electron level investigations, especially at electron level. How the 3d and 4f electrons as well as spins influence the magnetic and catalytic performances is also mysterious and challenging. To solve this problem, extensive work should be conducted. Firstly, to design and fabricate specific nanostructure directed by the application demand is crucial. This may be achieved by the optimization of the existing synthesis method and exploration into the new synthesis method. Secondly, atom structure and electron structure should be quantitatively studied and the result should be related to a single building block, i.e. nanoparticles, nanowires and nanotubes, instead of the average effect of their aggregations. It can be realized with the development in the characterization techniques such as XPS, TEM, synchrotron radiation, etc. Especially with the help of advanced TEM techniques, i.e. ACEM, in-situ TEM, Electron Magnetic Chiral Dichroism and time-resolved TEM, etc., the atomic structure as well as the electron structure of the MNs can be achieved quantitatively. Magnetic and catalytic behavior of the NMs can also be observed and investigated at atomic scale in the microscope. Moreover, combined with modeling and theoretical computation, the relationship between property and structure could be clearer and more credible.

Furthermore, problem for scale-up is an important issue for nanoscience, which makes it difficult to realize the industrialization. As the performance critically depends on the quality of the synthesized product, large-scale controllable synthesis of bimetallic NMs is another trend of future research. This may be realized by the new synthesis method based on the thorough investigation on the relationship between product quality and synthesis conditions.

Acknowledgments

The work is supported by the National Natural Science Foundation of China (Nos. 50971011 and 11174023), Beijing Natural Science Foundation (No. 1102025), and Research Fund for the Doctoral Program of Higher Education of China (No. 20091102110038).

References

[1] L.D. Marks, Experimental studies of small particle structures, Reports on Progress in Physics 57 (6) (1994) 603.
[2] J.D. Aiken III, R.G. Finke, A review of modern transition-metal nanoclusters: their synthesis, characterization, and applications in catalysis, Journal of Molecular Catalysis A: Chemical 145 (1–2) (1999) 1–44.
[3] A.-H. Lu, E.L. Salabas, F. Schueth, Magnetic nanoparticles: synthesis, protection, functionalization, and application, Angewandte Chemie-International Edition 46 (8) (2007) 1222–1244.
[4] K. Lu, The future of metals, Science 328 (5976) (2010) 319–320.
[5] C.N.R. Rao, G.U. Kulkarni, P.J. Thomas, P.P. Edwards, Metal nanoparticles and their assemblies, Chemical Society Reviews 29 (1) (2000) 27–35.
[6] N. Toshima, Recent progress in applications of ligand-stabilized metal nanoclusters, Macromolecular Symposia 204 (1) (2003) 219–226.
[7] J.P. Wilcoxon, B.L. Abrams, Synthesis, structure and properties of metal nanoclusters, Chemical Society Reviews 35 (11) (2006) 1162–1194.
[8] E. Roduner, Size matters: why nanomaterials are different, Chemical Society Reviews 35 (7) (2006) 583–592.
[9] S. Xiao, W. Hu, W. Luo, Y. Wu, X. Li, H. Deng, Size effect on alloying ability and phase stability of immiscible bimetallic nanoparticles, European Physical Journal B 54 (4) (2006) 479–484.
[10] S. Link, Z.L. Wang, M.A. El-Sayed, Alloy formation of gold–silver nanoparticles and the dependence of the plasmon absorption on their composition, Journal of Physical Chemistry B 103 (18) (1999) 3529–3533.
[11] K.J. Major, C. De, S.O. Obare, Recent advances in the synthesis of plasmonic bimetallic nanoparticles, Plasmonics 4 (1) (2009) 61–78.
[12] S.A. Chambers, Y.K. Yoo, New materials for spintronics, MRS Bulletin 28 (10) (2003) 706–708.
[13] J.A. Rodriguez, D.W. Goodman, The nature of the metal metal bond in bimetallic surfaces, Science 257 (5072) (1992) 897–903.
[14] J. Tanori, N. Duxin, C. Petit, I. Lisiecki, P. Veillet, M.P. Pileni, Synthesis of nanosize metallic and alloyed particles in ordered phases, Colloid and Polymer Science 273 (9) (1995) 886–892.
[15] Q.J. Ge, Y.M. Huang, F.Y. Qiu, S.B. Li, Bifunctional catalysts for conversion of synthesis gas to dimethyl ether, Applied Catalysis A—General 167 (1) (1998) 23–30.
[16] F. Massicot, R. Schneider, Y. Fort, S. Illy-Cherrey, O. Tillement, Synergistic effect in bimetallic ni-al clusters. Application to efficient catalytic reductive dehalogenation of polychlorinated arenes, Tetrahedron 56 (27) (2000) 4765–4768.
[17] M.O. Nutt, J.B. Hughes, M.S. Wong, Designing Pd-on-Au bimetallic nanoparticle catalysts for trichloroethene hydrodechlorination, Environmental Science & Technology 39 (5) (2005) 1346–1353.
[18] R.T. Mu, Q.A. Fu, H. Xu, H.I. Zhang, Y.Y. Huang, Z. Jiang, S.O. Zhang, D.L. Tan, X.H. Bao, Synergetic effect of surface and subsurface ni species at Pt–Ni bimetallic catalysts for CO oxidation, Journal of the American Chemical Society 133 (6) (2011) 1978–1986.
[19] N.S. Sobal, U. Ebels, H. Mohwald, M. Giersig, Synthesis of core–shell PtCo nanocrystals, Journal of Physical Chemistry B 107 (30) (2003) 7351–7354.
[20] D. Kodama, K. Shinoda, K. Sato, Y. Konno, R.J. Joseyphus, K. Motomiya, H. Takahashi, T. Matsumoto, Y. Sato, K. Tohji, B. Jeyadevan, Chemical synthesis of sub-micrometer- to nanometer-sized magnetic feco dice, Advanced Materials 18 (23) (2006) 3154–3159.
[21] T. Hyeon, Chemical synthesis of magnetic nanoparticles, Chemical Communications 8 (2003) 927–934.
[22] K.-M. Kang, H.-W. Kim, I.-W. Shim, H.-Y. Kwak, Catalytic test of supported Ni catalysts with core/shell structure for dry reforming of methane, Fuel Processing Technology 92 (6) (2011) 1236–1243.
[23] N. Semagina, L. Kiwi-Minsker, Recent advances in the liquid-phase synthesis of metal nanostructures with controlled shape and size for catalysis, Catalysis Reviews-Science and Engineering 51 (2) (2009) 147–217.
[24] R. Sardar, A.M. Funston, P. Mulvaney, R.W. Murray, Gold nanoparticles: past, present, and future, Langmuir 25 (24) (2009) 13840–13851.
[25] M.N. Nadagouda, R.S. Varma, A greener synthesis of core (Fe, Cu)–shell (An, Pt, Pd, and Ag) nanocrystals using aqueous vitamin C, Crystal Growth & Design 7 (12) (2007) 2582–2587.

[26] M. Mannini, F. Pineider, P. Sainctavit, C. Danieli, E. Otero, C. Sciancalepore, A.M. Talarico, M.A. Arrio, A. Cornia, D. Gatteschi, R. Sessoli, Magnetic memory of a single-molecule quantum magnet wired to a gold surface, Nature Materials 8 (3) (2009) 194–197.
[27] F. Tao, M.E. Grass, Y.W. Zhang, D.R. Butcher, J.R. Renzas, Z. Liu, J.Y. Chung, B.S. Mun, M. Salmeron, G.A. Somorjai, Reaction-driven restructuring of Rh–Pd and Pt–Pd core–shell nanoparticles, Science 322 (5903) (2008) 932–934.
[28] D. Fox, R. Verre, B.J. O'dowd, S.K. Arora, C.C. Faulkner, I.V. Shvets, H. Zhang, Investigation of coupled cobalt–silver nanoparticle system by plan view TEM, Progress in Natural Science: Materials International 22 (3) (2012) 186–192.
[29] R. Ferrando, J. Jellinek, R.L. Johnston, Nanoalloys: from theory to applications of alloy clusters and nanoparticles, Chemical Reviews 108 (3) (2008) 845–910.
[30] D.S. Wang, Y.D. Li, Bimetallic nanocrystals: liquid-phase synthesis and catalytic applications, Advanced Materials 23 (9) (2011) 1044–1060.
[31] Z. Peng, H. Yang, Synthesis and oxygen reduction electrocatalytic property of Pt-on-Pd bimetallic heteronanostructures, Journal of the American Chemical Society 131 (22) (2009) 7542–7543.
[32] D. Wang, Y. Li, One-pot protocol for Au-based hybrid magnetic nanostructures via a noble-metal-induced reduction process, Journal of the American Chemical Society 132 (18) (2010) 6280–6281.
[33] D.Y. Wang, H.L. Chou, Y.C. Lin, F.J. Lai, C.H. Chen, J.F. Lee, B.J. Hwang, C.C. Chen, Simple replacement reaction for the preparation of ternary $Fe_{1-x}PtRu_x$ nanocrystals with superior catalytic activity in methanol oxidation reaction, Journal of the American Chemical Society 134 (24) (2012) 10011–10020.
[34] M.S. Chen, D. Kumar, C.W. Yi, D.W. Goodman, The promotional effect of gold in catalysis by palladium–gold, Science 310 (5746) (2005) 291–293.
[35] J. Zhang, J.-O. Mueller, W. Zheng, D. Wang, D. Su, R. Schloegl, Individual Fe–Co alloy nanoparticles on carbon nanotubes: structural and catalytic properties, Nano Letters 8 (9) (2008) 2738–2743.
[36] S. Anandan, F. Grieser, M. Ashok kumar, Sonochemical synthesis of Au–Ag core–shell bimetallic nanoparticles, Journal of Physical Chemistry C 112 (39) (2008) 15102–15105.
[37] K.E. Elkins, T.S. Vedantam, J.P. Liu, H. Zeng, S.H. Sun, Y. Ding, Z.L. Wang, Ultrafine FePt nanoparticles prepared by the chemical reduction method, Nano Letters 3 (12) (2003) 1647–1649.
[38] J.-M. Yan, X.-B. Zhang, T. Akita, M. Haruta, Q. Xu, One-step seeding growth of magnetically recyclable Au@Co core-shell nanoparticles: highly efficient catalyst for hydrolytic dehydrogenation of ammonia borane, Journal of the American Chemical Society 132 (15) (2010) 5326–5327.
[39] M. Tsuji, D. Yamaguchi, M. Matsunaga, K. Ikedo, Epitaxial growth of Au@Ni core–shell nanocrystals prepared using a two-step reduction method, Crystal Growth & Design 11 (5) (2011) 1995–2005.
[40] Q. Sun, Z. Ren, R.M. Wang, N. Wang, X. Cao, Platinum catalyzed growth of NiPt hollow spheres with an ultrathin shell, Journal of Materials Chemistry 21 (6) (2011) 1925–1930.
[41] Q. Sun, W. Liu, R.M. Wang, Double-layered NiPt nanobowls with ultrathin shell synthesized in water at room temperature, CrystEngComm 14 (16) (2012) 5151–5154.
[42] Y.Y. Jiang, Y.Z. Lu, D.X. Han, Q.X. Zhang, L. Niu, Hollow Ag@Pd core–shell nanotubes as highly active catalysts for the electro-oxidation of formic acid, Nanotechnology 23 (10) (2012) 105609.
[43] H.M. Chen, C.F. Hsin, P.Y. Chen, R.S. Liu, S.F. Hu, C.Y. Huang, J.F. Lee, L.Y. Jang, Ferromagnetic $CoPt_3$ nanowires: structural evolution from fcc to ordered L1(2), Journal of the American Chemical Society 131 (43) (2009) 15794–15801.
[44] C.Z. Zhu, S.J. Guo, S.J. Dong, PdM (M=Pt, Au) bimetallic alloy nanowires with enhanced electrocatalytic activity for electro-oxidation of small molecules, Advanced Materials 24 (17) (2012) 2326–2331.
[45] S.J. Hurst, E.K. Payne, L.D. Qin, C.A. Mirkin, Multisegmented one-dimensional nanorods prepared by hard-template synthetic methods, Angewandte Chemie-International Edition 45 (17) (2006) 2672–2692.
[46] W. Wei, S. Li, J.E. Millstone, M.J. Banholzer, X. Chen, X. Xu, G.C. Schatz, C.A. Mirkin, Surprisingly long-range surface-enhanced Raman scattering (SERS) on Au–Ni multisegmented nanowires, Angewandte Chemie-International Edition 48 (23) (2009) 4210–4212.
[47] J.R. Choi, S.J. Oh, H. Ju, J. Cheon, Massive fabrication of free-standing one-dimensional Co/Pt nanostructures and modulation of ferromagnetism via a programmable barcode layer effect, Nano Letters 5 (11) (2005) 2179–2183.
[48] C. Wang, Y. Hou, J. Kim, S. Sun, A general strategy for synthesizing FePt nanowires and nanorods, Angewandte Chemie-International Edition 46 (33) (2007) 6333–6335.
[49] X. Hong, D. Wang, R. Yu, H. Yan, Y. Sun, L. He, Z. Niu, Q. Peng, Y. Li, Ultrathin Au–Ag bimetallic nanowires with coulomb blockade effects, Chemical Communications 47 (18) (2011) 5160–5162.
[50] S.H. Sun, C.B. Murray, D. Weller, L. Folks, A. Moser, Monodisperse FePt nanoparticles and ferromagnetic FePt nanocrystal superlattices, Science 287 (5460) (2000) 1989–1992.
[51] W.L. Zhou, E.E. Carpenter, J. Lin, A. Kumbhar, J. Sims, C.J. O'connor, Nanostructures of gold coated iron core–shell nanoparticles and the nanobands assembled under magnetic field, European Physical Journal D 16 (1–3) (2001) 289–292.
[52] Y. Lu, Y. Zhao, L. Yu, L. Dong, C. Shi, M.-J. Hu, Y.-J. Xu, S.-H. Wen L-Pyu, Hydrophilic Co@Au yolk/shell nanospheres: synthesis, assembly, and application to gene delivery, Advanced Materials 22 (12) (2010) 1407–1411.
[53] P.W. Li, W.M. Chen, W. Liu, Z.A. Li, Y.M. Cui, A.P. Huang, R.M. Wang, C.P. Chen, Thermodynamic phase formation of morphology and size controlled Ni nanochains by temperature and magnetic field, Journal of Physical Chemistry C 114 (17) (2010) 7721–7726.
[54] P.W. Li, Y.M. Cui, G. Behan, H.Z. Zhang, R.M. Wang, Room temperature synthesis and one-dimensional self-assembly of interlaced Ni nanodiscs under magnetic field, Journal of Physics D-Applied Physics 43 (27) (2010) 275002.
[55] P.W. Li, R.M. Wang, W.M. Chen, C.P. Chen, X.Y. Gao, A.T.S. Wee, Well-aligned nickel nanochains synthesized by a template-free route, Nanoscale Research Letters 5 (3) (2010) 597–602.
[56] P.W. Li, N. Wang, R.M. Wang, Flower-like nickel nanocrystals: facile synthesis, shape evolution, and their magnetic properties, European Journal of Inorganic Chemistry 15 (2010) 2261–2265.
[57] R.M. Wang, P.W. Li, C.P. Chen, Template-free synthesis and self-assembly of aligned nickel nanochains under magnetic fields, Journal of Nanoscience and Nanotechnology 11 (12) (2011) 11128–11132.
[58] Q. Sun, S.G. Wang, R.M. Wang, Well-aligned CoPt hollow nanochains synthesized in water at room temperature, Journal of Physical Chemistry C 116 (9) (2012) 5352–5357.
[59] M.E. Gruner, G. Rollmann, P. Entel, M. Farle, Multiply twinned morphologies of FePt and CoPt nanoparticles, Physical Review Letters 100 (8) (2008) 087203.
[60] D. Alloyeau, C. Ricolleau, C. Mottet, T. Oikawa, C. Langlois, Y. Le Bouar, N. Braidy, A. Loiseau, Size and shape effects on the order–disorder phase transition in CoPt nanoparticles, Nature Materials 8 (12) (2009) 940–946.
[61] P. Strasser, S. Koh, T. Anniyev, J. Greeley, K. More, C. Yu, Z. Liu, S. Kaya, D. Nordlund, H. Ogasawara, M.F. Toney,

A. Nilsson, Lattice-strain control of the activity in dealloyed core–shell fuel cell catalysts, Nature Chemistry 2 (6) (2010) 454–460.
[62] H. Luo, R. Jing, Y.-M. Cui, H.-L. Wang, R.M. Wang, Improvement of fabrication precision of focused ion beam by introducing simultaneous electron beam, Progress in Natural Science: Materials International 20 (0) (2010) 111–115.
[63] K. Sun, J. Liu, N.K. Nag, N.D. Browning, Atomic scale characterization of supported Pd–Cu/γ-Al_2O_3 bimetallic catalysts, Journal of Physical Chemistry B 106 (47) (2002) 12239–12246.
[64] K.W. Urban, Studying atomic structures by aberration-corrected transmission electron microscopy, Science 321 (5888) (2008) 506–510.
[65] M.J. Hytch, J.L. Putaux, J.M. Penisson, Measurement of the displacement field of dislocations to 0.03 angstrom by electron microscopy, Nature 423 (6937) (2003) 270–273.
[66] M. Hytch, F. Houdellier, F. Hue, E. Snoeck, Nanoscale holographic interferometry for strain measurements in electronic devices, Nature 453 (7198) (2008) 1086–1090.
[67] A. Mayoral, S. Mejia-Rosales, M.M. Mariscal, E. Perez-Tijerina, M. Jose-Yacaman, The Co–Au interface in bimetallic nanoparticles: a high resolution stem study, Nanoscale 2 (12) (2010) 2647–2651.
[68] B. Lim, J.G. Wang, P.H.C. Camargo, M.J. Jiang, M.J. Kim, Y.N. Xia, Facile synthesis of bimetallic nanoplates consisting of Pd cores and Pt shells through seeded epitaxial growth, Nano Letters 8 (8) (2008) 2535–2540.
[69] D. Ferrer, D.A. Blom, L.F. Allard, S. Mejia, E. Perez-Tijerina, M. Jose-Yacaman, Atomic structure of three-layer Au/Pd nanoparticles revealed by aberration-corrected scanning transmission electron microscopy, Journal of Materials Chemistry 18 (21) (2008) 2442–2446.
[70] R.M. Wang, O. Dmitrieva, M. Farle, G. Dumpich, H.Q. Ye, H. Poppa, R. Kilaas, C. Kisielowski, Layer resolved structural relaxation at the surface of magnetic FePt icosahedral nanoparticles, Physical Review Letters 100 (1) (2008) 017205.
[71] R.M. Wang, H.Z. Zhang, M. Farle, C. Kisielowski, Structural stability of icosahedral FePt nanoparticles, Nanoscale 1 (2) (2009) 276–279.
[72] R.M. Wang, O. Dmitrieva, M. Farle, G. Dumpich, M. Acet, S. Mejia-Rosales, E. Perez-Tijerina, M.J. Yacaman, C. Kisielowski, FePt icosahedra with magnetic cores and catalytic shells, Journal of Physical Chemistry C 113 (11) (2009) 4395–4400.
[73] N. Braidy, Z.J. Jakubek, B. Simard, G.A. Botton, Quantitative energy dispersive X-ray microanalysis of electron beam-sensitive alloyed nanoparticles, Microscopy and Microanalysis 14 (2) (2008) 166–175.
[74] L.F. Allard, W.C. Bigelow, M. Jose-Yacaman, D.P. Nackashi, J. Damiano, S.E. Mick, A new MEMS-based system for ultra-high-resolution imaging at elevated temperatures, Microscopy Research and Technique 72 (3) (2009) 208–215.
[75] B. Lim, H. Kobayashi, P.H.C. Camargo, L.F. Allard, J. Liu, Y. Xia, New insights into the growth mechanism and surface structure of palladium nanocrystals, Nano Research 3 (3) (2010) 180–188.
[76] A. Cao, G. Veser, Exceptional high-temperature stability through distillation-like self-stabilization in bimetallic nanoparticles, Nature Materials 9 (1) (2010) 75–81.
[77] S.H. Sun, C.B. Murray, Synthesis of monodisperse cobalt nanocrystals and their assembly into magnetic superlattices (invited), Journal of Applied Physics 85 (8) (1999) 4325–4330.
[78] F. Baletto, C. Mottet, R. Ferrando, Reentrant morphology transition in the growth of free silver nanoclusters, Physical Review Letters 84 (24) (2000) 5544–5547.
[79] H.G. Lang, S. Maldonado, K.J. Stevenson, B.D. Chandler, Synthesis and characterization of dendrimer templated supported bimetallic Pt–Au nanoparticles, Journal of the American Chemical Society 126 (40) (2004) 12949–12956.
[80] P. Mulvaney, Surface plasmon spectroscopy of nanosized metal particles, Langmuir 12 (3) (1996) 788–800.
[81] A.K. Salem, P.C. Searson, K.W. Leong, Multifunctional nanorods for gene delivery, Nature Materials 2 (10) (2003) 668–671.
[82] A.E. Pullen, S. Zeltner, R.-M. Olk, E. Hoyer, K.A. Abboud, J.R. Reynolds, Electrically conducting materials based on μ-tetrathiooxalato-bridged bimetallic Ni(II) anionic complexes, Inorganic Chemistry 36 (19) (1997) 4163–4171.
[83] S. Zhao, R.J. Gorte, The activity of Fe–Pd alloys for the water–gas shift reaction, Catalysis Letters 92 (1) (2004) 75–80.
[84] V. Abdelsayed, G. Glaspell, M. Nguyen, J.M. Howe, M. Samy El-Shall, Laser synthesis of bimetallic nanoalloys in the vapor and liquid phases and the magnetic properties of PdM and PtM nanoparticles (M = Fe, Co and Ni), Faraday Discussions 138 (2008) 163–180.
[85] P. Yu, M. Pemberton, P. Plasse, PtCo/C cathode catalyst for improved durability in PEMFCs, Journal of Power Sources 144 (1) (2005) 11–20.
[86] V.V. Temnov, G. Armelles, U. Woggon, D. Guzatov, A. Cebollada, A. Garcia-Martin, J.M. Garcia-Martin, T. Thomay, A. Leitenstorfer, R. Bratschitsch, Active magneto-plasmonics in hybrid metal–ferromagnet structures, Nature Photonics 4 (2) (2010) 107–111.
[87] B. Sepulveda, A. Calle, L.M. Lechuga, G. Armelles, Highly sensitive detection of biomolecules with the magneto-optic surface-plasmon-resonance sensor, Optics Letters 31 (8) (2006) 1085–1087.
[88] H. Coufal, L. Dhar, C.D. Mee, Materials for magnetic data storage: the ongoing quest for superior magnetic materials, MRS Bulletin 31 (5) (2006) 374–375.
[89] D. Zhang, R. Chung, A.B. Karki, F. Li, D.P. Young, Z. Guo, Magnetic and magnetoresistance behaviors of solvent extracted particulate iron/polyacrylonitrile nanocomposites, Journal of Physical Chemistry C 114 (1) (2010) 212–219.
[90] Z. Guo, S. Park, H.T. Hahn, S. Wei, M. Moldovan, A.B. Karki, D.P. Young, Giant magnetoresistance behavior of an iron/carbonized polyurethane nanocomposite, Applied Physics Letters 90 (2007) 053111.
[91] R.C. Che, L.M. Peng, X.F. Duan, Q. Chen, X.L. Liang, Microwave absorption enhancement and complex permittivity and permeability of Fe encapsulated within carbon nanotubes, Advanced Materials 16 (5) (2004) 401–405.
[92] Y.J. Chen, P. Gao, C.L. Zhu, R.X. Wang, L.J. Wang, M.S. Cao, X.Y. Fang, Synthesis, magnetic and electromagnetic wave absorption properties of porous Fe_3O_4/Fe/SiO_2 core/shell nanorods, Journal of Applied Physics 106 (2009) 5.
[93] M.P. Pileni, Magnetic fluids: fabrication, magnetic properties, and organization of nanocrystals, Advanced Functional Materials 11 (5) (2001) 323–336.
[94] H. Bonnemann, R.A. Brand, W. Brijoux, H.W. Hofstadt, M. Frerichs, V. Kempter, W. Maus-Friedrichs, N. Matoussevitch, K.S. Nagabhushana, F. Voigts, V. Caps, Air stable Fe and Fe–Co magnetic fluids—synthesis and characterization, Applied Organometallic Chemistry 19 (6) (2005) 790–796.
[95] C. Sun, J.S.H. Lee, M.Q. Zhang, Magnetic nanoparticles in MR imaging and drug delivery, Advanced Drug Delivery Reviews 60 (11) (2008) 1252–1265.
[96] P.S. Doyle, J. Bibette, A. Bancaud, J.L. Viovy, Self-assembled magnetic matrices for DNA separation chips, Science 295 (5563) (2002) 2237.
[97] Z.H. Lu, M.D. Prouty, Z.H. Guo, V.O. Golub, C. Kumar, Y.M. Lvov, Magnetic switch of permeability for polyelectrolyte microcapsules embedded with Co@Au nanoparticles, Langmuir 21 (5) (2005) 2042–2050.
[98] T. Yamauchi, Y. Tsukahara, K. Yamada, T. Sakata, Y. Wada, Nucleation and growth of magnetic Ni–Co (core–shell) nanoparticles in a one-pot reaction under microwave irradiation, Chemistry of Materials 23 (1) (2011) 75–84.

[99] M. Gottwald, S. Andrieu, F. Gimbert, E. Shipton, L. Calmels, C. Magen, E. Snoeck, M. Liberati, T. Hauet, E. Arenholz, S. Mangin, E.E. Fullerton, Co/Ni(111) superlattices studied by microscopy, X-ray absorption, and ab initio calculations, Physical Review B 86 (1) (2012) 014425.
[100] B. Lu, H. Huang, X.L. Dong, X.F. Zhang, J.P. Lei, J.P. Sun, C. Dong, Influence of alloy components on electromagnetic characteristics of core/shell-type Fe–Ni nanoparticles, Journal of Applied Physics 104 (11) (2008) 114313.
[101] N.O. Nunez, P. Tartaj, M.P. Morales, P. Bonville, C.J. Serna, Yttria-coated FeCo magnetic nanoneedles, Chemistry of Materials 16 (16) (2004) 3119–3124.
[102] C. Wang, S. Peng, L.-M. Lacroix, S. Sun, Synthesis of high magnetic moment CoFe nanoparticles via interfacial diffusion in core/shell structured Co/Fe nanoparticles, Nano Research 2 (5) (2009) 380–385.
[103] A.K. Giri, K.M. Chowdary, S.A. Majetich, Ac magnetic properties of compacted FeCo nanocomposites, Materials Physics and Mechanics 1 (1) (2000) 1–10.
[104] X. Li, Y.-X. Duan, Y. Zhao, L. Zhu, Effects of heat treatment on magnetic properties of Co–Fe-plated hollow ceramic microspheres, Progress in Natural Science: Materials International 21 (5) (2011) 392–400.
[105] Z. Turgut, N.T. Nuhfer, H.R. Piehler, M.E. Mchenry, Magnetic properties and microstructural observations of oxide coated FeCo nanocrystals before and after compaction, Journal of Applied Physics 85 (8) (1999) 4406–4408.
[106] O. Crisan, M. Angelakeris, N.K. Flevaris, G. Filoti, Magnetism and anisotropy in core–shell nanoparticles, Journal of Optoelectronics and Advanced Materials 5 (4) (2003) 959–962.
[107] J.I. Park, M.G. Kim, Y.W. Jun, J.S. Lee, W.R. Lee, J. Cheon, Characterization of superpararnagnetic core–shell nanoparticles and monitoring their anisotropic phase transition to ferromagnetic solid solution nanoalloyse, Journal of the American Chemical Society 126 (29) (2004) 9072–9078.
[108] S.C. Tsang, N. Cailuo, W. Oduro, A.T.S. Kong, L. Clifton, K.M.K. Yu, B. Thiebaut, J. Cookson, P. Bishop, Engineering preformed cobalt-doped platinum nanocatalysts for ultraselective hydrogenation, ACS Nano 2 (12) (2008) 2547–2553.
[109] F. Zheng, S. Alayoglu, J.H. Guo, V. Pushkarev, Y.M. Li, P.A. Glans, J.L. Chen, G. Somorjai, In-situ x-ray absorption study of evolution of oxidation states and structure of cobalt in Co and CoPt bimetallic nanoparticles (4 nm) under reducing (H_2) and oxidizing (O_2) environments, Nano Letters 11 (2) (2011) 847–853.
[110] L. Wang, Y. Yamauchi, Autoprogrammed synthesis of triple-layered Au@Pd@Pt core–shell nanoparticles consisting of a Au@Pd bimetallic core and nanoporous Pt shell, Journal of the American Chemical Society 132 (39) (2010) 13636–13638.
[111] J. Chen, J.M. Mclellan, A. Siekkinen, Y. Xiong, Z.-Y. Li, Y. Xia, Facile synthesis of gold–silver nanocages with controllable pores on the surface, Journal of the American Chemical Society 128 (46) (2006) 14776–14777.
[112] L. Au, X. Lu, Y. Xia, A comparative study of galvanic replacement reactions involving Ag nanocubes and $AuCl_2$ or $AuCl_4$, Advanced Materials 20 (13) (2008) 2517–2522.
[113] P.-P. Fang, J.-F. Li, Z.-L. Yang, L.-M. Li, B. Ren, Z.-Q. Tian, Optimization of SERS activities of gold nanoparticles and gold-core–palladium-shell nanoparticles by controlling size and shell thickness, Journal of Raman Spectroscopy 39 (11) (2008) 1679–1687.
[114] Y. Yang, J.L. Shi, G. Kawamura, M. Nogami, Preparation of Au–Ag, Ag–Au core–shell bimetallic nanoparticles for surface-enhanced Raman scattering, Scripta Materialia 58 (10) (2008) 862–865.

Rongming Wang received his Bachelor (1994) and Master's (1994) Degrees in Physics from Peking University and Ph. D. (1997) in Materials Science from Beijing Institute of Aeronautical Materials (BIAM), China. From 1997-2002, he was a senior engineer at BIAM with short period post-doctoral experience in Ben-Gurion University at Negev, Israel in 2000. Then he joined Peking University as an associate professor. In 2004-2005, he was a visiting scholar in Lawrence Berkeley National Laboratory, University of California, Berkeley. In Oct. 2005, he joined Beijing University of Aeronautics and Astronautics as a Professor in physics. His research interests include the synthesis, atomic structure and properties of metallic and semiconducting nanomaterials and their low dimensional physical properties.